J Physiol 589.21 (2011) pp 5071–5089

The Journal of Physiology

Two-pore domain K^+ channels regulate membrane potential of isolated human articular chondrocytes

Robert B. Clark, Colleen Kondo, Darrell D. Belke and Wayne R. Giles

Roger Jackson Centre for Health and Wellness Research, Faculty of Kinesiology, University of Calgary, Calgary, Alberta, Canada T2N 4N1

Non-technical summary The debilitating condition of arthritis is caused by degeneration of the cartilage, a tissue that allows almost frictionless motion between the ends of bones in articulating joints such as the knee. The integrity of the cartilage is maintained by the metabolic activity of chondrocytes, the only type of cell found within the cartilage. An important factor in regulating the rate of metabolic activity of the chondrocytes is thought to be the magnitude of the electrical potential difference across the cell membrane, i.e. the 'membrane potential'. This study identifies a type of ion channel, a so-called 'two-pore potassium channel', which was not previously known to be expressed in human chondrocytes. This ion channel importantly contributes to controlling chondrocyte membrane potential. Elucidation of the factors that control chondrocyte membrane potential is important for understanding the normal and pathophysiology of the chondrocytes, and consequently the health of the cartilage.

Abstract Potassium channels that regulate resting membrane potential (RMP) of human articular chondrocytes (HACs) of the tibial joint maintained in short-term (0–3 days) non-confluent cell culture were studied using patch-clamp techniques. Quantitative PCR showed that transcripts of genes for two-pore domain K^+ channels (*KCNK1*, *KCNK5* and *KCNK6*), and 'BK' Ca^{2+}-activated K^+ channels (*KCNMA1*) were abundantly expressed. Immunocytological methods detected α-subunits for BK and $K_{2p}5.1$ (TASK-2) K^+ channels. Electrophysiological recordings identified three distinct K^+ currents in isolated HACs: (i) a voltage- and time-dependent 'delayed rectifier', blocked by 100 nM α-dendrotoxin, (ii) a large 'noisy' voltage-dependent current that was blocked by low concentrations of tetraethylammonium (TEA; 50% blocking dose = 0.15 mM) and iberiotoxin (52% block, 100 nM) and (iii) a voltage-independent 'background' K^+ current that was blocked by acidic pH (5.5–6), was increased by alkaline pH (8.5), and was not blocked by TEA, but was blocked by the local anaesthetic bupivacaine (0.25 mM). The RMP of isolated HACs was very slightly affected by 5 mM TEA, which was sufficient to block both voltage-dependent K^+ currents, suggesting that these currents probably contributed little to maintaining RMP under 'resting' conditions (i.e. low internal $[Ca^{2+}]$). Increases in external K^+ concentration depolarized HACs by 30 mV in response to a 10-fold increase in $[K^+]$, indicating a significant but not exclusive role for K^+ current in determining RMP. Increases in external $[K^+]$ in voltage-clamped HACs revealed a voltage-independent K^+ current whose inward current magnitude increased with external $[K^+]$. Block of this current by bupivacaine (0.25–1 mM) in 5 and 25 mM external $[K^+]$ resulted in a large (8–25 mV) depolarization of RMP. The biophysical and pharmacological properties of the background K^+ current, together with expression of mRNA and α-subunit protein for TASK-2, strongly suggest that these two-pore domain K^+ channels contribute significantly to stabilizing the RMP of HACs.

(Received 15 April 2011; accepted after revision 8 September 2011; first published online 12 September 2011)
Corresponding author W. R. Giles: Faculty of Kinesiology, University of Calgary, Calgary, Alberta, Canada T2N 4N1. Email: wgiles@ucalgary.ca

Abbreviations: AC, articular chondrocyte; ECM, extracellular matrix; HAC, human articular chondrocyte; RMP, resting membrane potential.

DOI: 10.1113/jphysiol.2011.210757

Introduction

Chondrocytes, the sole cellular component of mature articular cartilage, are responsible for the production of extracellular matrix (ECM) constituents such as proteoglycans, collagen and non-collagenous proteins, thereby maintaining the integrity and physio-chemical properties of the cartilage (Fassbender, 1987; Muir, 1995). Metabolism of ECM constituents by chondrocytes has been shown to be sensitive to intracellular ionic concentrations in these cells (Eilam *et al.* 1985; Gray *et al.* 1988; Urban *et al.* 1993; Wilkins & Hall, 1995). The repertoire of ion channels in chondrocyte cell membrane (Barrett-Jolley *et al.* 2010) undoubtedly plays a central role in maintaining intracellular ionic homeostasis via transmembrane ion fluxes. Cellular membrane potential, which arises from the balance of ion fluxes through active channels in the surface membrane, has a significant influence on the magnitude and direction of the ionic fluxes and thus can indirectly influence chondrocyte metabolism. The observation that ion channel blockers that may modify membrane potential result in reduced matrix mRNAs (Wu & Chen, 2000), and protein and sulfated glycoaminoglycans (Mouw *et al.* 2007) support this idea. Additionally, ion channel blockers such as lidocaine, bupivacaine and verapamil inhibit HAC proliferation (Wohlrab *et al.* 2001, 2005) and increase apoptosis and mitochondrial dysfunction (Grishko *et al.* 2010). For these reasons determining the contributions(s) of various ion channels to establishing chondrocyte membrane potential and intracellular ionic homeostasis is essential for an understanding of the normal and pathophysiology of articular chondrocytes and cartilage.

Potassium channels play a major role in generating the membrane potential of most animal cells. Electrophysiological studies have identified several types of K^+ channels in mammalian chondrocyte surface membranes, including voltage-gated 'delayed-rectifier', Ca^{2+}-activated, ATP-sensitive, and stretch-activated (for reviews see Mobasheri *et al.* 2008; Barrett-Jolley *et al.* 2010). Some of these K^+ channels have been demonstrated to have an important role in generating the resting membrane potential (RMP) of chondrocytes. For example, acutely isolated canine articular chondrocytes express a voltage-gated 'delayed-rectifier' K^+ current which is inhibited by the non-specific K^+ channel blockers tetraethylammonium (TEA) and 4-aminopyridine (4-AP) (Wilson *et al.* 2004). Block of the K^+ current by TEA results in concomitant depolarization of the chondrocytes. Similar delayed-rectifier K^+ currents were recorded from rat (Ponce, 2006) and neonatal mouse (Clark *et al.* 2010) articular chondrocytes, and pharmacological block of these K^+ currents produced significant membrane depolarization of chondrocytes of both species. Rat chondrocytes were significantly depolarized by α-dendrotoxin, which blocks a delayed-rectifier K^+ current in these cells. A similar delayed rectifier K^+ current is blocked in mouse articular chondrocytes by low concentrations of α-dendrotoxin. Measurements of expression levels of a number of voltage-gated K^+ channel genes suggest that Kv1.6 K^+ channels, an important target for α-dendrotoxin, are primarily responsible for generating the 'delayed-rectifier' K^+ current of mouse cells. Other studies have implicated Ca^{2+}-activated K^+ channels in generation of membrane potential of chondrocytes, especially following mechanical stress or stimulation of hormone receptors. For example, membrane hyperpolarization of HACs occurs in response to repetitive mechanical stimulation, and this hyperpolarization is inhibited by apamin, a blocker of 'small conductance' SK Ca^{2+}-activated K^+ channels (Wright *et al.* 1996). Histamine increases intracellular Ca^{2+} concentration in OUMS-27 cell line human chondrocytes, resulting in membrane hyperpolarization due to activation of three different types of Ca^{2+}-activated K^+ channels (Funabashi *et al.* 2010*b*).

Two-pore domain K^+ channels (K_{2p}) are a very widely expressed family of 15 related K^+-selective channels (Goldstein *et al.* 2005). Unlike most other K^+ channels, which are tetrameric combinations of α-subunits containing a single pore-forming 'P loop', each α-subunit of K_{2p} channels contains two P loops and only two α-subunits associate to form the ion channel. In contrast to many other types of K^+ channels, activation of many types of K_{2p} channels is largely independent of membrane potential. Hence K_{2p} ion channels underlie the quasi-instantaneous background 'leak' K^+ currents observed in many types of excitable and non-excitable cells. The activity of K_{2p} channels is modulated by a wide variety of chemical and physical stimuli, with different members of the K_{2p} family responding to extra- or intracellular pH, temperature, membrane stretch, fatty acids, G-protein-coupled receptors and local and volatile anaesthetics (see Lesage & Lazdunski, 2000; Goldstein *et al.* 2001; Patel & Honoré, 2001; Kindler & Yost, 2005 for reviews). Thus, K_{2p} K^+ channels can serve as a highly adaptable and sensitive substrate for control of membrane potential in response to changes in the extra- and intracellular environments of a wide variety of mammalian cells.

This study is the first report showing that several types of two-pore domain K^+ channels are expressed in adult HACs in short-term primary cell culture. Quantitative RT-PCR showed consistent expression of transcripts of three *KCNK* genes, namely *KCNK1*, *KCNK5* and *KCNK6*, which correspond to TWIK-1, TASK-2 and TWIK-2 K_{2p} K^+ channels, respectively. Electrophysiological recordings from isolated HACs identified K^+ currents with biophysical and pharmacological properties most consistent with those of TASK-2 K_{2p} currents, and

these K^+ currents were shown to contribute significantly to the membrane potential of the chondrocytes. These findings and previous literature suggest that K_{2p} channels are important for regulating the membrane potential of chondrocytes in response to physiological changes in their extracellular environment such as K^+ concentration, pH and osmolality, in the intact cartilage.

Methods

Cells and cell culture

Samples of cartilage from the plateau of the tibial condyle of deceased donors were obtained through the Southern Alberta Organ and Tissue Donation Program. Use of the tissue conformed to the ethical requirements of the Conjoint Health Research Ethics Board of the Faculties of Medicine, Nursing and Kinesiology, University of Calgary and the Affiliated Teaching Institutions. These ethical requirements conformed to the *Declaration of Helsinki*. Samples were taken from areas of the cartilage that appeared grossly normal. Cartilage was obtained from nine male donors, aged 43 to 74 years (mean ± SEM: 60.1 ± 3.3 years) and one female donor, aged 31. Following collection the cartilage samples were refrigerated at 4°C for up to 1 week prior to beginning cell isolation procedures.

Cartilage chips (~2 mm cubes) were placed in solution consisting of Dulbecco's modified Eagle's medium (DMEM)–F12 low glucose culture medium (Invitrogen/Gibco; Carlsbad, CA, USA) containing 5% fetal bovine serum (FBS; Gibco), 0.4 mM L-proline (Sigma-Aldrich; St Louis, MO, USA), 2 mM L-glutamine (Gibco), 0.1 mM minimal essential medium (MEM) non-essential amino acids (Sigma-Aldrich), penicillin–streptomycin 1% (Gibco) and fungizone 0.25 μg ml^{-1} (Gibco). Cartilage chips were initially digested in pronase Type XIV (Sigma-Aldrich) for 1.5 h at 37°C. Pronase solution was removed and further digestion continued with 15 h of incubation in collagenase P (1.25 mg (g tissue)$^{-1}$) (Boehringer Mannheim). At the end of this incubation period, cells were filtered with a 70 μm cell strainer, then washed with cold (4°C) phosphate-buffered saline (PBS; Gibco) and centrifuged 3 times (750 *g*; 5 min). After a final filtration with a 40 μm cell strainer, cells were placed in DMEM low glucose medium containing 10% FBS, 0.4 mM L-proline, 2.0 mM L-glutamine, 0.1 mM MEM non-essential amino acids, 10 mM Hepes (Gibco), and penicillin–streptomycin 1%.

Isolated cells were either plated immediately after isolation or were preserved for cryostorage at –80°C for up to 4 months before plating. An aliquot of solution containing (1–2) × 10^5 either freshly isolated or cryopreserved cells was plated into 2 ml of medium in a plastic 35 mm culture dish containing a number of pieces of glass coverslip. The culture dish was incubated in a 5% CO_2 atmosphere at 37°C. Cells were used between 6 and 72 h following isolation and plating.

Quantitative RT-PCR (qRT-PCR) for K^+ channel isoform expression in HACs

HAC mRNA expression levels of *KCNK1–6*, *KCNK9*, *KCNK10*, *KCNK13*, *KCNMA1*, *KCNJ4* and *KCNJ12* were determined using Quantitect human primer pairs obtained from Qiagen (Mississauga, ON, Canada). The Quantitect SYBR Green PCR kit was used in an iCycler (Bio-Rad; Hercules, CA, USA). Harvesting of mRNA from chondrocytes was accomplished with the Qiagen RNeasy extraction kit using the manufacturer's protocol for isolation from cultured cells. RNA isolated from the chondrocytes was converted to cDNA using the Quantitect Reverse Transcription kit from Qiagen according to the manufacturer's directions. Quantitative real time PCR was performed using the SYBR Green PCR kit according to the manufacturer's protocol with 18S RNA serving as the housekeeping reference gene for determining the expression levels of the individual mRNA species. Samples were measured in triplicate for each individual gene, with relative expression levels being calculated using the $\Delta\Delta C_T$ method. Cells were harvested following identical culture conditions to those used for the electrophysiological experiments. Transcripts were measured separately on samples of HACs from four different donors, and the results were pooled. The age of these donors ranged from 31 to 63 years (mean = 46.8 ± 6.7 years: 1 ♀, 31 years; 3 ♂, 43, 50 and 63 years).

Single cell immunocytological identification of K^+ channel α-subunits

Chondrocytes plated on glass coverslips for 1 or 2 days were fixed with 2% paraformaldehyde for 30 min at room temperature. Fixed cells were rinsed three times with PBS (Gibco) and permeabilized with 10% goat serum (Sigma-Aldrich) in PBS and 0.2% Triton X-100 for 20 min at room temperature. The cells were rinsed three times in 1% goat serum in PBS, then incubated overnight (~12 h) at 4°C with anti-KNCMA1 rabbit polyclonal antibody (Millipore; Billerica, MA, USA), diluted 1:500, or anti-KCNK5 rabbit polyclonal antibody (Abcam; Cambridge, MA, USA), diluted 1:500. The cells were rinsed three times in PBS and then incubated for at least 1 h at room temperature in 1% goat serum PBS containing Alexa Fluor 568 (KCNK5) or Alexa Fluor 488 (KCNMA1) goat anti-rabbit IgG (Molecular Probes/Invitrogen), diluted 1:200. Images were taken on a Zeiss Axiovision LSM 7 DUO confocal microscope. Alexa Fluor 568 was excited at 543 nm; emission spectra were recorded between 568 and 712 nm. Alexa Fluor 488 was excited at 489 nm,

and emission spectra were recorded between 493 and 630 nm. Images were acquired and analysed using Zeiss ZEN software.

Electrophysiology

Pieces of coverslip from a culture dish were placed in a recording chamber on an inverted microscope, and were superfused with a Hepes-buffered solution at a rate of about 1 ml min^{-1}. Rapid (∼1–2 s) solution changes around single cells were made with a solenoid-controlled, multi-barrel local superfusion device. Temperature was 20–22°C.

Whole-cell 'patch clamp' was used to measure membrane potential and currents from single chondrocytes. Single, isolated cells with a round or ovoid morphology and with minimal spreading on the glass substrate were chosen for these electrophysiological studies. Patch pipettes were pulled from borosilicate glass capillaries and the tips lightly fire-polished. The pipettes had a DC resistance of 5–8 MΩ when filled with 'intracellular' solution. Mean (±SEM; $n = 169$) resistance of the 'on-cell' seal before breaking into the cell was 42.0 ± 1.3 GΩ (range: 8.8–105.1 GΩ). Recordings of current and membrane potential were made with a Multi-Clamp 700A patch clamp amplifier (Molecular Devices; Sunnyvale, CA, USA). Ten millivolts was subtracted from membrane potentials recorded by the patch-clamp amplifier in order to compensate for the liquid junction potential between the bath and pipette solutions (Neher, 1992). Signals were digitized with a 1322A Digi-Data acquisition system (Molecular Devices), stored on a microcomputer, and analysed offline with pCLAMP v. 8. Plots, statistical analysis and curve-fitting were done with commercial software, 'Sigmaplot' (Systat Software; San Jose, CA, USA) or 'Prism' (GraphPad Software; La Jolla, CA, USA).

Current–voltage (I–V) relations of cells were determined using either 'step' or 'ramp' voltage-clamp protocols. The 'step' protocol consisted of a series of 1 s rectangular voltage steps, applied at 0.2 Hz, over the range from –130 mV to +90 mV, generally from a holding potential of –90 mV. I–V relations were constructed from the magnitude of membrane current *vs.* potential. Because the currents were (i) noisy at some potentials, and (ii) showed little inactivation during the voltage steps, current was averaged in the time window between 400 and 600 ms of the step. The 'ramp' protocol consisted of a 1 s voltage ramp, from –110 or –150 mV to +140 mV, from a holding potential of –90 mV. Voltage ramps were applied at a rate of 0.2 Hz. Currents at selected potentials during ramps were measured by averaging the current in a 5 mV window centred on the potential. Recordings were not compensated for 'leakage' currents. Recordings of RMP were 'noisy', especially for 'low' external concentrations of K^+, e.g. 5 mM. Mean RMP was determined by averaging values in 10–20 s time windows.

Cell capacitance was measured from the area of the current transient produced by a +5 mV step from a holding potential of –90 mV. When data from groups of cells were pooled, membrane currents from each cell were normalized to their respective capacitance ('current density') before averaging. The capacitance of freshly isolated HAC was slightly larger than that of cryopreserved cells. The mean capacitance of 128 freshly isolated cells, in culture between 6 to 72 h, was 8.1 ± 0.3 pF, somewhat larger than the mean capacitance of 234 cryopreserved cells in culture for the same length of time, 7.1 ± 0.2 pF ($P = 2.6 \times 10^{-3}$; unpaired t test, with Welch's correction for unequal variances).

Solutions, chemicals, drugs

Analar grade chemicals (Sigma-Aldrich) were used to make solutions. Tetraethylammonium (TEA) chloride and bupivacaine were obtained from Sigma-Aldrich. The snake toxin α-dendrotoxin (α-DTX), and the scorpion toxin iberiotoxin (IbTX) were obtained from Alomone Labs (Jerusalem, Israel). 'Standard' external solution consisted of (mM): NaCl, 140; KCl, 5; $CaCl_2$, 2; $MgCl_2$, 1; Hepes, 10; glucose, 5.5; mannitol, 15. pH was adjusted to 7.4 with NaOH. Solution osmolality was measured with a freezing-point depression osmometer (Model 3250; Advanced Inst., Norwood, MA, USA), and was in the range 300–310 mosmol kg^{-1}. In experiments where external K^+ concentration was changed, appropriate volumes of modified external solutions with 145 mM NaCl–0 KCl and 145 mM KCl–0 NaCl were mixed to obtain the desired K^+ concentration. The concentrations of $CaCl_2$, $MgCl_2$, glucose, Hepes and mannitol in these solutions were the same as in 'standard' solution. 'Internal' (pipette) solution consisted of (mM): potassium aspartate, 100; KCl, 20; $MgCl_2$, 1; Na_2ATP, 4; $CaCl_2$, 0.85; EGTA, 5; Hepes, 10. pH was adjusted to 7.2 with KOH. Osmolality of this solution was 284–287 mosmol kg^{-1}. The approximate pCa of the solution was 7.9.

Statistics

Averaged data are shown as means ± standard error of the mean (SEM). Matched or unmatched values were tested for statistical differences using Student's t test or ANOVA as appropriate. A P value of <0.05 was taken to indicate a statistically significant difference.

Results

Expression of K^+ channels in HACs measured with qRT-PCR and immunocytology

Expression levels of 12 K^+ channel genes in isolated, cell cultured HACs were measured using qRT-PCR. Figure 1*A* shows that three *KCNK* genes, namely *KCNK1*, *KCNK5* and *KCNK6*, were expressed at significant levels in HAC under the same cell isolation and culture conditions as those used in the electrophysiological recordings. The expression levels of six other *KCNK* genes, *KCNK2*, *KCNK3*, *KCNK4*, *KCNK9*, *KCNK10* and *KCNK13*, were very small or virtually undetectable. Two-pore domain K^+ (K_{2p}) channels are the protein product of *KCNK* genes, suggesting that such K^+ channels are expressed in HACs under our conditions. The three *KCNK* genes expressed in abundance in HACs correspond to TWIK-1 (*KNCK1*), TASK-2 (*KCNK5*) and TWIK-2 (*KCNK6*) K_{2p} K^+ channels. *KCNMA1*, corresponding to the α-subunit of the large conductance Ca^{2+}-activated K^+ channel, BK, was highly expressed in HACs. *KCNJ4* and *KCNJ12* correspond to the strong inwardly rectifying K^+ channels Kir2.3 and Kir2.2, respectively. There was negligible expression of *KCNJ4*, but a very small expression of *KCNJ12* was detected.

The data shown in Fig. 1*A* were obtained from four different donors: qRT-PCR was performed separately on populations of cells from each of the four donors and the results were then averaged. Although there was quantitative variability in the level of expression of each of the 12 K^+ channel transcripts amongst the different donors, the donor-to-donor expression of the K^+ channel genes was qualitatively consistent, particularly for the nine *KCNK* transcripts.

Immunocytological data (Fig. 1*B*) showed that protein corresponding to α-subunits for BK and TASK-2 K^+ channels was abundantly expressed in cell-cultured HACs. The cells shown in Fig. 1*B* were cultured for 1 day (TASK-2) or 2 days (BK). The cells exhibited some spreading on the glass substrate after 2 days of culture; however, expression of both BK and TASK-2 K^+ channels was observed to be independent of cell morphology. Only single cells with a round or elliptical shape that were not in visible contact with any neighbouring cells were used for electrophysiology. Fluorescence was absent if Alexa Fluor-labelled secondary antibodies were applied without

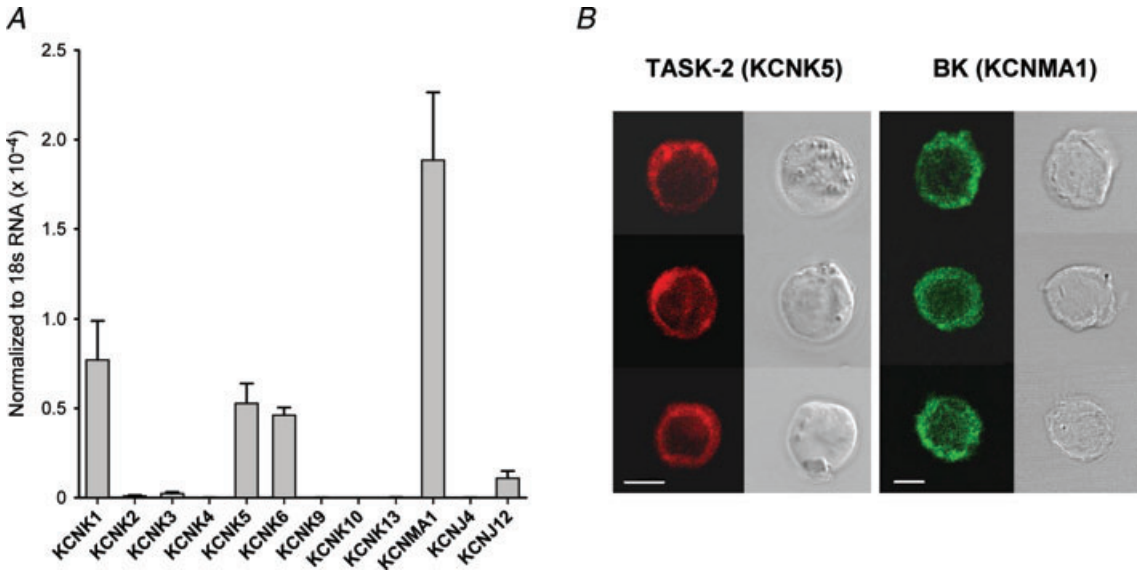

Figure 1 Expression of selected K^+ channel genes and α-subunits in HACs
A,expression levels of transcripts of K^+ channel genes in isolated HAC, determined using qRT-PCR. mRNA levels of each gene were normalized to 18S mRNA levels. Three of nine KCNK genes were expressed at readily detectable levels. *KCNMA1*, corresponding to large conductance Ca^{2+}-activated, 'BK' K^+ channel, was expressed at high levels. Genes for two inwardly rectifying K^+ channels (*KCNJ*) were expressed at low or negligible levels. Data were pooled from 4 different donors. *B*, immunocytological evidence for expression of TASK-2 (*KCNK5*) and BK (*KCNMA1*) K^+ channel α-subunits in isolated HACs. Cells were in culture for 1 day (TASK-2) or 2 days (BK). Three different HACs are shown for each antibody. The fluorescence image as shown in the left columns; the corresponding differential interference contrast image of each cell is shown at right. The calibration bar corresponds to 5 μm.

the primary antibodies for BK and TASK-2 α-subunits (data not shown).

Current–voltage (*I–V*) relation of HACs

Figure 2*A* shows a representative example of the *I–V* relation of a HAC, produced by a step voltage-clamp protocol. The currents were recorded in 'control' conditions with external pH of 7.4, low internal free Ca^{2+} concentration (pCa nominally 7.9) and 5 mM external K^+. Several properties of the currents and the *I–V* are of note. Currents produced by potential steps between –130 mV and approximately –50 mV were very small and inward. In contrast, currents for steps positive to –40 mV were net outward and their magnitudes increased more than linearly with increasing depolarization up to the maximum of +90 mV used in the protocol. This resulted in very pronounced outward rectification of the *I–V* relation (see also Fig. 2*B*). In approximately 50% (26 of 50) of the cells, steps between –40 mV and +50 mV exhibited currents with 'delayed rectifier' properties, namely time- and voltage-dependent activation. The properties of this delayed rectifier current are most evident in the current records in Fig. 2*A* for voltage steps between –40 mV and +10 mV. It is apparent from these records that the magnitude and the rate of activation of the current greatly increased as membrane potential was more depolarized.

In almost all cells, currents for steps positive to about +50 mV exhibited large fluctuations or 'noise', the amplitude of which steeply increased with increasing depolarization (Fig. 2*A*). The mean step *I–V* (current density) relation for 50 HACs (from 5 different donors) is shown in Fig. 2*B*. The mean capacitance of the group of 50 cells was 8.50 ± 0.42 pF. The zero-current potential of the mean *I–V* relation was –46.9 mV. The *I–V* relation between –130 and –50 mV was linear, and corresponded to a mean apparent input resistance of 11.2 ± 1.2 GΩ ($n = 50$). The very high apparent input resistance of HACs is similar to that recorded from isolated canine (Wilson *et al.* 2004) and neonatal mouse (Clark *et al.* 2010) articular chondrocytes under very similar conditions.

'Noisy' outward current is sensitive to tetraethylammonium (TEA) and iberiotoxin (IbTX)

The non-selective K^+ channel blocker TEA blocked the 'noisy' component of outward current in HACs at relatively low concentrations. Figure 3*A* shows currents recorded first in control conditions, then from the same cell in the presence of 0.25 mM TEA. Similar to the data shown in Fig. 2*A*, this cell expressed both a time- and voltage-dependent delayed rectifier current and a 'noisy' outward current with large fluctuations. Application of 0.25 mM TEA to this cell greatly reduced the mean magnitude and the amplitude of the fluctuations of the 'noisy' component of current. The delayed rectifier current in contrast was only slightly reduced by the low concentration of TEA.

The magnitude of the TEA-sensitive component of outward current was very strongly dependent on

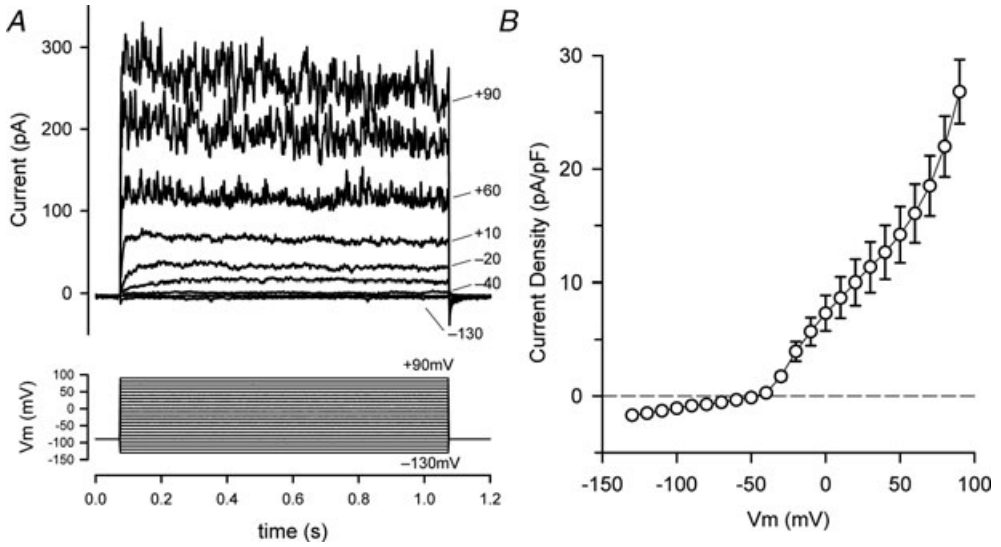

Figure 2. Current-voltage (*I–V*) relation for HACs
A, superimposed currents (upper panel) produced by a 'step' voltage-clamp protocol (lower panel) in a HAC. The protocol consisted of twenty-three 1 s steps from a holding potential of –90 mV, to potentials between –130 and +90 mV. Steps were applied at a rate of 0.2 Hz. For clarity, only currents for steps to –130, –90, –40, –30, –20, +10, +60, +80 and +90 mV are shown; some of these are labelled. Cell capacitance was 7.9 pF. *B*, mean *I–V* relation, pooled from data from 50 different HACs. Current for each cell was normalized to cell capacitance (current density) before averaging. Mean capacitance = 8.5 ± 0.42 pF.

membrane potential. This is shown in Fig. 3*B*, where the *I–V* voltage-clamp protocol consisted of a voltage 'ramp' (see Methods), rather than a series of steps. The ramp extended to considerably more positive potentials than the step protocol, namely +140 mV *vs.* +90 mV, respectively, which resulted in very large outward currents during the ramp protocol. Figure 3*B* compares *I–V* relations generated by ramp voltage-clamp protocols in control conditions, and in the presence of 0.25 and 2.5 mM TEA. These data were obtained from the same cell as in Fig. 3*A*. Note that consistent with the step *I–V* data shown in Fig. 3*A*, 0.25 mM TEA blocked only about 50% of the outward current at +140 mV, while the 10-fold higher concentration blocked about 85% of the net outward current. The inset to Fig. 3*B* shows the dose–response relation for inhibition of outward current (at +140 mV) by TEA obtained from eight different HACs. Current magnitudes for each cell were normalized to control conditions, and the normalized currents at each TEA concentration were averaged. The mean data were fitted to an equation of the form:

$$I = \frac{I_s}{1 + [\mathrm{TEA}]/K} + I_i$$

where I is the normalized current, I_s is the fraction of current sensitive to TEA, I_i is the fraction of current that is insensitive to TEA, and K is the 50% blocking concentration of TEA. The parameters for best-fit of this equation to the averaged dose–response data in Fig. 3*C* were $I_s = 0.91$ (± 0.007), $I_i = 0.09$ (± 0.004) and $K = 0.152$ mM (± 0.004). Hence about 90% of the outward current (at +140 mV) was sensitive to TEA, and 50% of the TEA-sensitive current was blocked by about 150 μM of TEA.

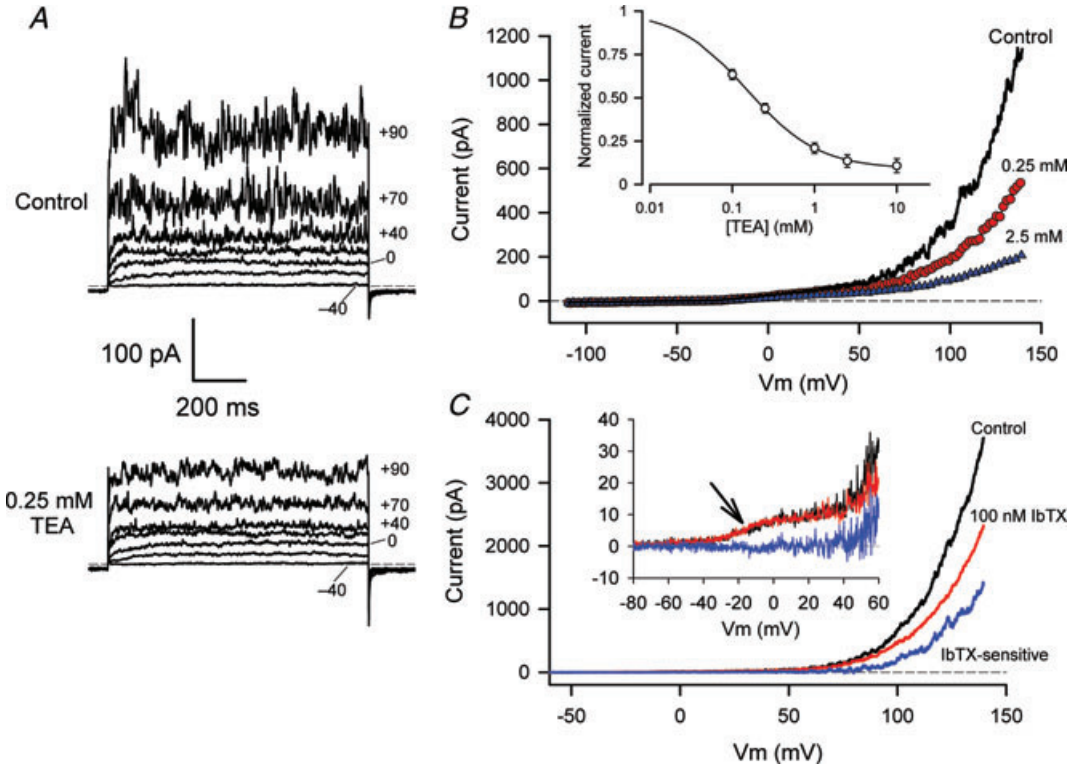

Figure 3. Block of HAC currents by tetraethylammonium (TEA)
A, currents produced by selected potential steps (voltages indicated) in a HAC in control conditions (upper panel), and in the presence of 0.25 mM TEA-Cl (lower panel). Current and time calibrations apply to both sets of currents. Dashed line indicates the zero current level. Cell capacitance was 7.1 pF. *B*, *I–V* relations were produced by a ramp voltage-clamp protocol, in control conditions, and in the same cell in the presence of 0.25 and 2.5 mM TEA, as indicated. The voltage-clamp protocol consisted of a 1 s ramp from –110 mV to +140 mV, from a holding potential of –90 mV. Inset: dose–response relation for the block of outward current (at +140 mV) by TEA. Current magnitudes for each of seven cells were normalized to control currents at each [TEA], and then averaged. The continuous line was fitted to the data as described in the text. *C*, block of voltage-clamp currents in a HAC by 100 nM iberiotoxin (IbTX). *I–V* relations were generated with a ramp protocol in control conditions (black) and in the presence of 100 nM IbTX (red). The IbTX-sensitive difference current (blue) begins to activate near +50 mV, and is negligible at more negative potentials. Inset: currents from a different HAC, in control (black) and 100 nM IbTX (red). The IbTX-sensitive current is shown in blue. Arrow indicates the presence of a voltage-dependent delayed rectifier current in this cell, which is insensitive to IbTX.

The large outward current component of HACs was partially blocked by 100 nM IbTX, a specific blocker of large conductance Ca^{2+}-activated BK K^+ channels. For five cells, the outward current at +140 mV was reduced by 52 ± 3%. Figure 3*C* illustrates that there was no IbTX-sensitive current at membrane potentials less positive than about +50 mV. The data in Fig. 3*C* also illustrate the selectivity of blocking of membrane currents in HACs by IbTX. The cell shown in the inset to Fig. 3*C* exhibited a small voltage-dependent delayed rectifier current which began to activate at about –40 mV, but this current was unaffected by IbTX. Taken together, the relatively high sensitivity of the large outward current in HACs to TEA and IbTX, and robust expression of gene transcripts underlying BK channels (*KCNMA1*) and protein for the α-subunit of the channel (Fig. 1), strongly suggest that the large, noisy TEA-sensitive current in HACs is produced by BK K^+ channels.

α-Dendrotoxin (α-DTX) blocks the delayed rectifier current of HACs

The data in Fig. 3 showed that the time and voltage-dependent delayed rectifier current in HACs was much less sensitive to TEA than the BK current. However, the snake toxin α-DTX was a potent and selective blocker of the delayed rectifier current. Figure 4*A* compares the effects of 0.25 mM TEA and 100 nM α-DTX on membrane currents of a voltage-clamped HAC. Similar to the data in Fig. 3*A*, 0.25 mM TEA significantly reduced the magnitude of the BK current with little effect on the delayed rectifier. Application of 100 nM of α-DTX to the same cell, however, resulted in selective block of the delayed rectifier current, without obvious effect on the BK current. Figure 4*B* shows the effect of 125 nM α-DTX on step *I–V* relations over a wide range of membrane potentials for 16 different HACs that expressed a delayed rectifier. These data were obtained in the presence of 0.25 mM TEA, which significantly blocked the large BK currents at depolarized potentials (e.g. Fig. 3*A*: 0.25 mM TEA). These *I–V* relations clearly show that α-DTX blocked a portion of the outward current in these HACs beginning at membrane potentials between –35 and –40 mV, potentials at which the time-dependent currents first appeared to activate. Assuming that the α-DTX-sensitive current is a K^+ current, a Boltzmann function was used to describe the membrane potential dependence of activation of the current (Fig. 4*C*) viz:

$$I = \frac{G_K(V_m - E_K)}{1 + \exp[-(V_m - V_h)/S_h)}$$

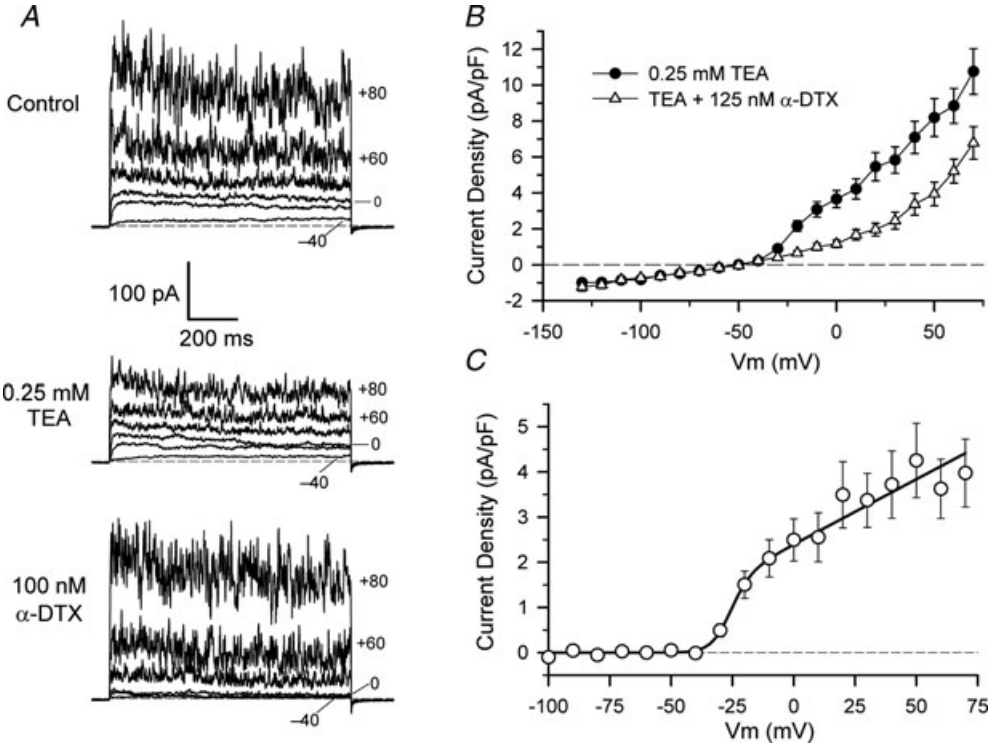

Figure 4. Block of HAC currents by α-dendrotoxin (α-DTX)
A, comparison of the effects of 0.25 mM TEA (middle panel) and 100 nM α-DTX (lower panel) on membrane currents of a HAC. Currents produced by potential steps to –40, –20, 0, +40, +60 and +80 mV are shown (selected voltages are indicated). *B*, mean step *I–V* (current density) relations for 16 HACs, in the presence of 0.25 mM TEA (filled circles) and in the presence of TEA and 125 nM α-DTX (open triangles). *C*, best-fit of a Boltzmann function (see text) to the α-DTX-sensitive current.

where G_K is maximal conductance, E_K is the Nernst potential (fixed at –83 mV, based on intracellular and extracellular K^+ concentrations), V_h is the potential for half-activation of the conductance, and S_h is a membrane potential sensitivity factor. Values of the parameters of the 'best-fit' line were $G_K = 28.9$ pS pF^{-1}, $V_h = -26.7$ mV and $S_h = 4.1$ mV. This equation indicates that on average the α-DTX-sensitive conductance began to activate near –40 mV, and was fully activated by about 0 mV.

Resting membrane potential of HACs

Previous studies have shown that the RMP of dog (Wilson *et al.* 2004), rat (Ponce, 2006) and neonatal mouse (Clark *et al.* 2010) articular chondrocytes is at least partly regulated by delayed rectifier K^+ currents. The possible involvement of delayed rectifier in contributing to RMP of HACs was tested by blocking this current with solutions containing TEA or TEA/α-DTX. Figure 5*A* shows an example of the effects of 5 mM TEA/100 nM

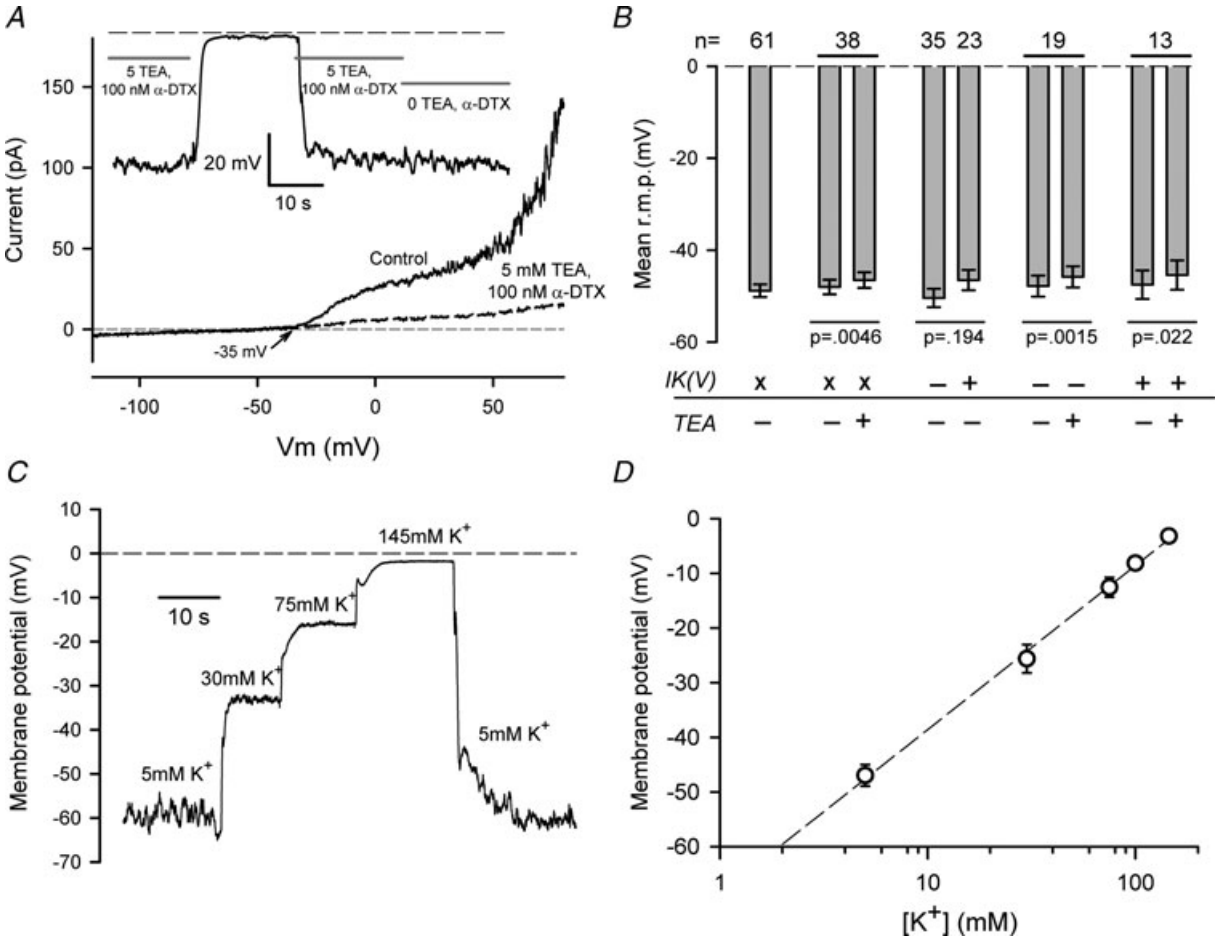

Figure 5. RMP of HACs
A, effect of 5 mM TEA and 100 nM α-DTX on membrane currents and RMP of a HAC. *I–V* relations produced by a ramp voltage-clamp protocol are shown before (Control; continuous line) and after exposure to 5 mM TEA/100 nM α-DTX (dashed line). Note complete inhibition of delayed rectifier and BK currents. Inset shows a continuous recording of RMP of the same cell when exposed to 5 mM K^+ solution with 5 mM TEA/100 nM α-DTX, or solution without these blockers, as indicated. (Between 15 and 35 s, the cell was exposed to 145 mM K^+/5 mM TEA.) Dashed line indicates 0 mV. *B*, summary of the effect of 5 mM TEA on RMP of HACs that did or did not express detectable delayed rectifier K^+ current. *n* values at top of graph show number of cells in each group. Paired treatments on the same group are indicated by horizontal lines. Statistical significance shown under bars are for paired or unpaired *t* test, as appropriate. 'x' indicates cell groups in which cells with and without delayed rectifier current (*IK*(*V*)) were mixed; '+' and '–' indicate groups with and without *IK*(*V*), respectively. See text for more detailed explanation. *C*, a continuous recording of RMP of a HAC in the presence of four concentrations of external K^+ (as indicated) is shown. Solution changes were made rapidly with a multi-barrel local superfusion device. *D*, plot of mean membrane potential *vs.* external [K^+]. Mean values were from 5–16 cells at each [K^+]. The dashed line is the best-fit of the equation RMP = $A + B \times \log([K^+])$, with $A = -68.6$ mV and $B = 30$ mV.

α-DTX on RMP and membrane currents of a HAC. This cell expressed a substantial delayed rectifier current that began to activate near –35 mV, and a large BK current that activated near +50 mV. Application of a solution containing 5 mM TEA/100 nM α-DTX blocked both outward currents. Also shown in Fig. 5*A* is a continuous recording of the RMP of the same cell during application of these solutions. It should be noted that there was no change in RMP when the solution containing TEA and α-DTX was switched to one without either K^+ channel blocker. Thus the delayed rectifier, and probably also BK K^+ currents, made no detectable contribution to the RMP of this HAC.

Figure 5*B* summarizes the results of similar experiments on groups of HACs. The mean RMP of 61 HACs in 5 mM external K^+ solution was –48.8 ± 1.4 mV. To test the possibility that delayed rectifier and/or BK K^+ currents contributed significantly to the RMP of HACs, RMP was recorded before and after application of 5 mM TEA, which blocked both of the K^+ currents as effectively as the TEA/α-DTX mixture. Because the measured RMP of HACs had a wide range, this test was done by comparing the RMP of the same groups of cells before and after application of K^+ current blockers. For a group of 38 cells, RMP before application of TEA averaged –48.0 ± 1.6 mV, and averaged –46.5 ± 1.7 mV for the same set of cells in the presence of 5 mM TEA (Fig. 5*B*). Although the mean depolarization produced by TEA was very small (1.4 mV), it was statistically significant in this group of cells ($P = 0.0046$). However, because not all HACs express a delayed rectifier K^+ current, it was necessary to compare the RMP of cells that expressed delayed rectifier with those that did not. A group of 35 cells that did not obviously express a delayed rectifier K^+ current had a mean RMP of –50.4 ± 2.0 mV, while the RMP of a group of 23 different cells that clearly expressed the current was –46.5 ± 2.2 mV. These mean values were not different ($P = 0.194$), suggesting the delayed rectifier current made very little, if any, contribution to RMP on average. The effect of 5 mM TEA on RMP was tested in two groups of cells that were separated on the basis of clear expression or lack of expression of delayed rectifier. For 19 cells lacking delayed rectifier, 5 mM TEA depolarized the cells from –47.8 ± 2.3 mV to –45.8 ± 2.3 mV ($P = 0.0015$), while 13 cells expressing the current were depolarized from –47.5 ± 3.1 mV to –45.4 ± 3.2 mV ($P = 0.022$). However, the small depolarizations produced by TEA in both groups of cells were not significantly different ($P = 0.558$) between the two groups. These RMP data are summarized in Fig. 5*B*. They strongly suggest that on average the delayed rectifier and BK K^+ currents do not contribute significantly to RMP of HACs, at least under our culture and recording conditions.

Dependence of resting membrane potential of HACs on external K^+ concentration

The zero-current potential of the *I–V* relation for HACs (Fig. 1*B*) suggested that the resting membrane potential (RMP) of HACs in 5 mM external K^+ was considerably more depolarized than the Nernst potential for K^+, which was about –83 mV in control recording conditions. Nevertheless, the RMP of isolated HACs was strongly dependent on external $[K^+]$. Figure 5*C* shows an example of the changes in RMP produced in one HAC by several concentrations of external K^+ over the range from 5 to 145 mM. This cell was depolarized by approximately 60 mV as external $[K^+]$ was changed from 5 to 145 mM. Figure 5*D* shows the relationship between RMP and external $[K^+]$ from data pooled from 5–16 different HACs. The line in Fig. 5*D* corresponds to a 30 mV depolarization of RMP with a 10-fold increase in external $[K^+]$. If RMP was produced solely by membrane K^+ permeability, RMP would change by about 58 mV for a 10-fold change in external $[K^+]$. The data in Fig. 5*D* indicate that although RMP of these isolated HACs is not determined exclusively by K^+ channels, they do make a very significant contribution to RMP. The sensitivity of the RMP of HACs to external $[K^+]$ is similar to that of rat articular chondrocytes, which were depolarized by 24 mV per 10-fold change in external $[K^+]$ (Ponce, 2006).

Elevated external $[K^+]$ reveals a time-independent 'background' K^+ current

The inward current of HACs in 5 mM external K^+ was very small (e.g. Fig. 2), but increasing external K^+ concentration produced inward currents whose magnitude increased significantly with increased external K^+ concentration. Figure 6*A* shows the striking changes that occurred in membrane currents produced by selected voltage-clamp steps when external K^+ was increased from 5 to 145 mM. These changes were most obvious for the most negative potential steps. For example, in 5 mM external K^+, the voltage step to –130 mV produced a net inward current of only approximately –5 pA, but in 145 mM external K^+ the same step resulted in a much larger current (mean ~–60 pA) that had large fluctuations or 'noise'. Similarly, the net inward holding current at –90 mV, which was ~2–3 pA in 5 mM K^+, increased to a mean value of –38 pA in 145 mM K^+, and was very 'noisy'. The magnitude of the inward currents (and 'noise') in 145 mM K^+ decreased as the potential steps became more positive, and the current was almost abolished at 0 mV. The currents from the cell in Fig. 6*A* were recorded in the absence of blockers of the delayed rectifier and BK currents, so these currents may also have contributed slightly to the net changes in current observed in increased

external K^+. However, the delayed rectifier current was virtually absent from this cell, so the changes in inward current in elevated [K^+] cannot be attributed to this K^+ current. Similarly, because the BK current was activated only positive to +50 mV under the conditions of these experiments, it is unlikely that it contributed significantly to inward current changes. Figure 6*B* shows step *I–V* data pooled from seven cells, in 5 mM and 145 mM external K^+. As indicated by the records in Fig. 6*A*, elevated external [K^+] produced inward currents between –130 mV and approximately –9 mV, the zero-current potential of the *I–V* relation in 145 mM K^+. This zero-current potential was consistent with the RMP of HACs in 145 mM K^+, which was –3.2 mV (Fig. 5*D*).

Figure 6*C* shows an example of the changes in membrane currents in a HAC resulting from a range of different external [K^+]. *I–V* relations were generated using the ramp voltage-clamp protocol in the presence of external K^+ concentrations of 5, 30, 75 and 145 mM. Three features of the *I–V* relations that were dependent on the external concentration of K^+ are noteworthy: (i) the magnitude of the inward current increased, (ii) the zero-current potential of each *I–V* relation became more positive, and (iii) the slope conductance of the *I–V* relation at the zero-current potential increased as the concentration of external K^+ was increased. The slope conductance of the *I–V* relation at zero-current is a measure of the magnitude of net currents that determine

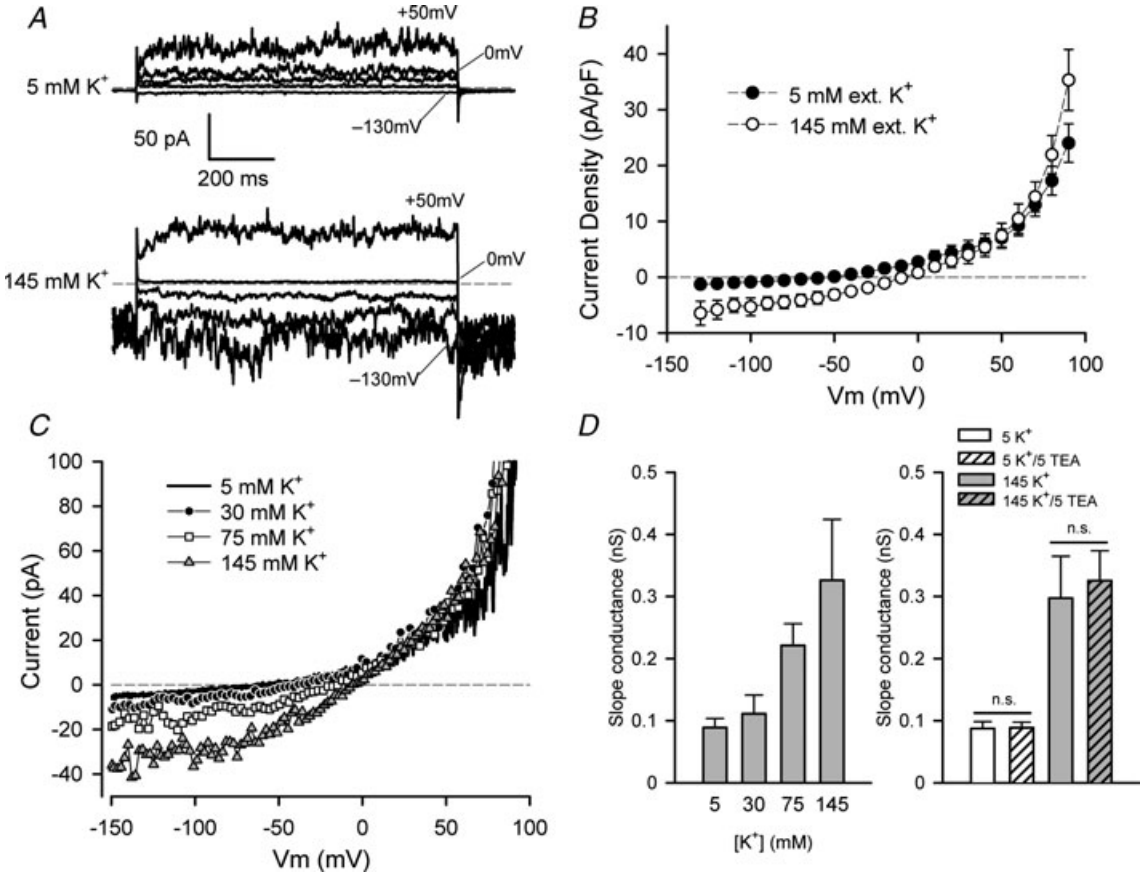

Figure 6. Effect of external [K^+] on the *I–V* relation of HACs
A, currents produced by voltage steps to –130, –50, –20, 0 and +50 mV (as indicated) in the same HACs in 5 mM external K^+ (upper panel) and in 145 mM K^+ (lower panel). Holding potential was –90 mV; note the large inward holding current in 145 mM K^+. Cell capacitance was 4.8 pF. *B*, mean step *I–V* (current density) relation from seven HACs, in 5 mM (filled circles) and 145 mM (open circles) external K^+. *C*, ramp *I–V* relations for same cell as in *A*, in 5, 30, 75 and 145 mM external K^+. Currents from three sweeps were averaged at each [K^+]. *D*, left-hand plot, mean slope conductance of ramp *I–V* (at the zero-current potential) *vs.* external [K^+]. A straight line was fitted to data points ±5 mV either side of the zero-current potential; the slope of the best-fit line was the slope conductance. $n = 5$ different HACs. Right-hand plot, mean slope conductance of ramp *I–V* (at zero-current potential) of HACs in 5 and 145 mM K^+, in the presence or absence of 5 mM TEA as indicated. For 5 mM K^+, $n = 24$; $P = 0.85$, paired *t* test. For 145 mM K^+, $n = 9$ without TEA, $n = 28$ with 5 mM TEA; $P = 0.76$, unpaired *t* test. 'n.s.' indicates not significantly different.

the RMP of the cell. The left-hand plot in Fig. 6*D* shows the relationship between external [K^+] and the slope conductance of the *I–V* relation at the zero-current potential in each [K^+], derived from ramp voltage-clamp currents similar to those shown in Fig. 6*C*. These data were pooled from five different cells. As shown by the currents in Fig. 6*C*, the slope conductance of the *I–V* was strongly dependent on external K^+ concentration, with an approximately threefold increase in conductance when [K^+] was increased from 5 to 145 mM. This concentration dependence of the zero-current potential and slope conductance of the *I–V* relation correlated with the dependence of RMP on external [K^+]. These findings provide strong evidence for an important role of this background K^+ current in contributing to the RMP of HACs.

The right-hand plot in Fig. 6*D* shows that this K^+ current was insensitive to 5 mM TEA. The plot shows the zero-current slope conductance of 9–28 HACs in 5 or 145 mM external K^+, in the presence or absence of 5 mM TEA. It is clear that the zero-current slope conductance was not affected by this concentration of TEA at either [K^+]. Similarly, inward currents in elevated external [K^+] were not affected by 5 mM TEA (data not shown.)

Background K^+ current is sensitive to external pH

Changing external pH (pH_o) had very significant effects on the background K^+ current. Figure 7*A* shows the effect on membrane current of changing pH_o, in the presence of 145 mM K^+. In this experiment, the cell was clamped at

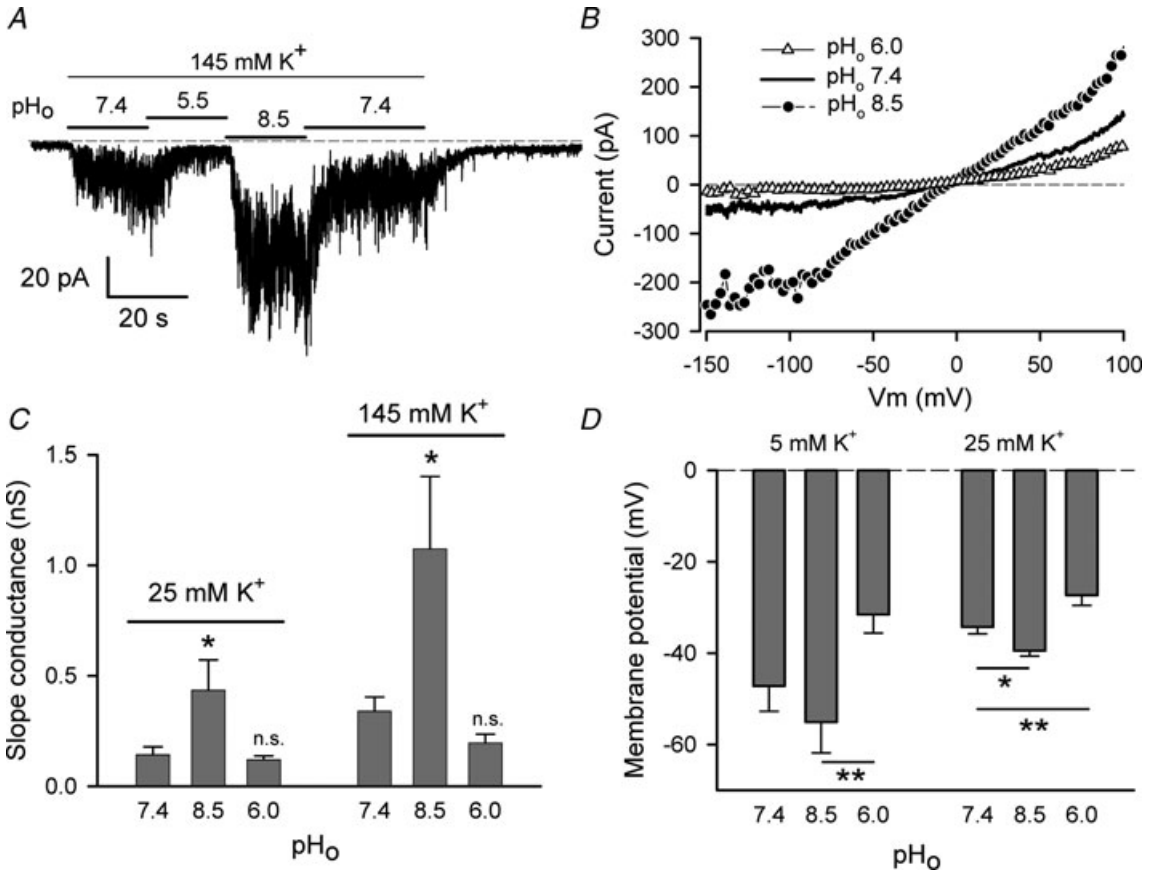

Figure 7. Effect of external pH (pH_o) on background K^+ current of HAC
A, currents recorded from a HAC voltage-clamped at a constant holding potential of –110 mV. The cell was initially in 5 mM K^+, pH_o 7.4, then the solution was switched to 145 mM K^+ at different pH_o, as indicated. *B*, ramp *I–V* relations in 145 mM K^+, at three different values of pH_o, as indicated (different cell from *A*). Currents were the average of three consecutive sweeps in each pH_o. Five millimolar TEA was added to all solutions. *C*, plots of zero-current slope conductance of the (ramp) *I–V*, in 25 and 145 mM external K^+, at three values of pH_o. Five millimolar TEA was included in all solutions. The 25 mM K^+ and 145 mM K^+ data were from 9 and 19 cells, respectively. Values are means ± SEM. $^*P < 0.05$, compared with pH_o 7.4 (repeated measures ANOVA). *D*, effect of pH_o on RMP of HAC in 5 and 25 mM external K^+. Solutions included 5 mM TEA for all recordings of RMP. Data were from 5 cells in 5 mM K^+ and 9 cells in 25 mM K^+. For 5 mM K^+, $^{**}P < 0.01$ for pH_o 8.5 *vs.* pH_o 6.0 (repeated measures ANOVA). For 25 mM K^+, $^*P < 0.05$ and $^{**}P < 0.01$, compared with pH_o 7.4 (repeated measures ANOVA), respectively.

a holding potential of –110 mV, and first exposed to the control solution, with 5 mM K^+ and pH_o of 7.4. External solution was switched to 145 mM K^+ for 90 s, during which pH_o was changed from 7.4 to 5.5 and 8.5 then back to 7.4, after which the solution was returned to the initial control solution. The magnitude of the current in 145 mM K^+ was very sensitive to pH_o, with acidic pH_o resulting in a very significant decrease in the current compared to its magnitude at pH_o 7.4, whereas alkaline pH_o greatly increased the current. The current in 145 mM K^+ was extremely 'noisy', similar to the step currents shown in Fig. 6*A*. Ramp *I–V* relations in 145 mM K^+, with different pH_o, are shown in Fig. 7*B*. The magnitude of both inward and outward limbs of the *I–V* relations were affected by pH_o. The *I–V* relations were recorded in the presence of 5 mM TEA at all pH_o, thus blocking both the delayed rectifier and BK K^+ currents. Figure 7*B* shows that changing pH_o altered the magnitude of the current at all membrane potentials. All of the currents crossed each other at approximately –2 mV, very close to the expected K^+ Nernst potential. Figure 7*C* shows the effect of pH_o on mean slope conductance for two external K^+ concentrations, 25 and 145 mM. The increase in pH_o from 7.4 to 8.5 resulted in a large increase in slope conductance at both external [K^+], an average of 3.04-fold for 25 mM K^+ and 3.16-fold for 145 mM K^+. There was, however, a large cell-to-cell variability in the increase in membrane currents (and hence conductance) induced by pH_o 8.5. For145 mM K^+ the increase in conductance on increasing pH_o from 7.4 to 8.5 ranged from 1.1- to 7.7-fold ($n = 19$ cells); for 25 mM K^+ the range was 1.2- to 4.2-fold ($n = 9$). The mean slope conductance at pH_o 6.0 was smaller than that for pH_o 7.4, but the difference was not statistically significant for the groups of cells in Fig. 7*C*, although the current was clearly inhibited in the majority of cells by acidic pH_o. For the cells used for Fig. 7*C*, 7/9 cells in 25 mM K^+ showed a reduced slope conductance in pH_o 6.0, while for 145 mM K^+, it was 14/19 cells.

As background K^+ current appeared to contribute significantly to RMP, it was expected that changes in magnitude of the current produced by changes in pH_o would alter RMP. That this was the case is shown in Fig. 7*D*. In 5 mM external K^+, increasing pH_o from 7.4 to 8.5 hyperpolarized RMP by 7.9 mV, while decreasing pH_o from 7.4 to 6.0 depolarized RMP by 15.7 mV. Although neither change in RMP was statistically significant with respect to pH_o 7.4, the 23.5 mV difference in RMP between pH_o 6.0 and 8.5 was highly significant ($P < 0.01$; repeated measures ANOVA, $n = 5$). In 25 mM K^+, mean RMP of nine cells hyperpolarized significantly from –34.3 mV in pH_o 7.4 to –39.5 mV in pH_o 8.5 ($P < 0.05$; repeated measures ANOVA). Decreasing pH_o for the same nine HACs from 7.4 to 6.0 depolarized the cells by an average of +6.9 mV, which was also statistically significant compared with RMP at pH_o of 7.4 ($P < 0.01$) and 8.5 ($P < 0.001$).

Pharmacological properties of background K^+ current

The local anaesthetic bupivacaine and the cations Ba^{2+} and Cs^+ blocked the background K^+ current in a voltage-dependent manner. This is shown in Fig. 8*A* for bupivacaine (at 0.25 mM), and in Fig. 8*C* and *D* for Ba^{2+} and Cs^+, respectively, both at a single concentration of 1 mM. Ramp protocols were used to generate the *I–V* relations in 145 mM external K^+ with pH_o of 8.5. It is clear from the data shown that the two cations and Bup had opposite voltage dependence of blocking. Bup blocked the K^+ current more strongly at positive membrane potentials; the percentage of block at +50 mV averaged approximately 67%, compared with approximately 46% at –150 mV ($n = 9$ cells). Conversely, 1 mM Ba^{2+} and Cs^+ blocked most strongly at negative membrane potentials. Ba^{2+} almost completely blocked the inward current at –150 mV, whereas the block was completely removed at +50 mV. Block of the current by Cs^+ was similarly strongest at negative membrane potentials and absent at positive potentials. The polarity of the voltage dependence of block by Ba^{2+} and Cs^+ suggests that the positively charged cations interact with open K^+ channels from the extracellular side of the membrane. Local anaesthetics such as bupivacaine are thought to interact with ion channels on the intracellular side of the cell membrane, in either a neutral or positively charged, protonated form. The opposite polarity of the voltage dependence of bupivacaine block suggests that an intracellularly located, protonated form of the drug at least partly contributed to blocking HAC background K^+ currents.

Block of the background K^+ current by Bup was expected to result in depolarization of HACs. Figure 8*B* shows the effect of 0.25 mM and 1 mM Bup on the RMP of HACs in 5 mM external K^+, and 0.25 mM Bup in 25 mM external K^+ (pH_o was 7.4 at both K^+ concentrations). Bup at 0.25 and 1 mM significantly depolarized HACs in 5 mM external K^+, by an average of 20.6 mV in 0.25 Bup and 24.6 mV in 1 mM Bup ($P < 0.001$ compared with control; $n = 8$), but there was no statistical difference ($P > 0.05$) in the depolarizations produced by the two concentrations of Bup. For 25 mM external K^+, 0.25 mM Bup produced an average depolarization of 8.3 mV ($P = 0.0127$; $n = 5$).

Discussion

This study demonstrates that adult HACs express two-pore domain background K^+ (K_{2p}) channels in addition to voltage-gated and Ca^{2+}-activated K^+ channels, and that the K_{2p} channels contribute significantly to the resting membrane potential of isolated HACs in short-term cell culture. This conclusion is based on the following evidence:

(1) Quantitative RT-PCR showed that mRNA for three *KCNK* genes, namely *KCNK1*, *KCNK5* and *KCNK6*,

was expressed at substantial levels in isolated HACs. Immunocytological data also demonstrated expression of TASK-2 (*KCNK5*) α-subunit protein in isolated HACs.

(2) Changes in external K^+ concentration revealed a time-independent background K^+ current whose amplitude was greatly increased by elevated pH_o.

(3) A 10-fold change in external $[K^+]$ produced a 30 mV change in RMP of the HACs. Changes in external pH altered RMP; acidification (pH 6.0) depolarized the cells, while alkalization (pH 8.5) produced hyperpolarization.

(4) The K^+ current was blocked in a membrane potential-dependent manner by the cations Ba^{2+} and Cs^+, and the local anaesthetic bupivacaine. Block of the current by bupivacaine significantly depolarized the cells.

K_{2p} channels should therefore be added to the types of K^+ channels that have been identified in other mammalian articular chondrocytes which includes voltage-, Ca^{2+}-, nucleotide- and stretch-activated K^+ channels (Mobasheri *et al.* 2008).

Voltage-gated K^+ channels in human articular chondrocytes

Under the recording conditions of these electrophysiological experiments, in particular low internal $[Ca^{2+}]$, membrane currents produced by two types of

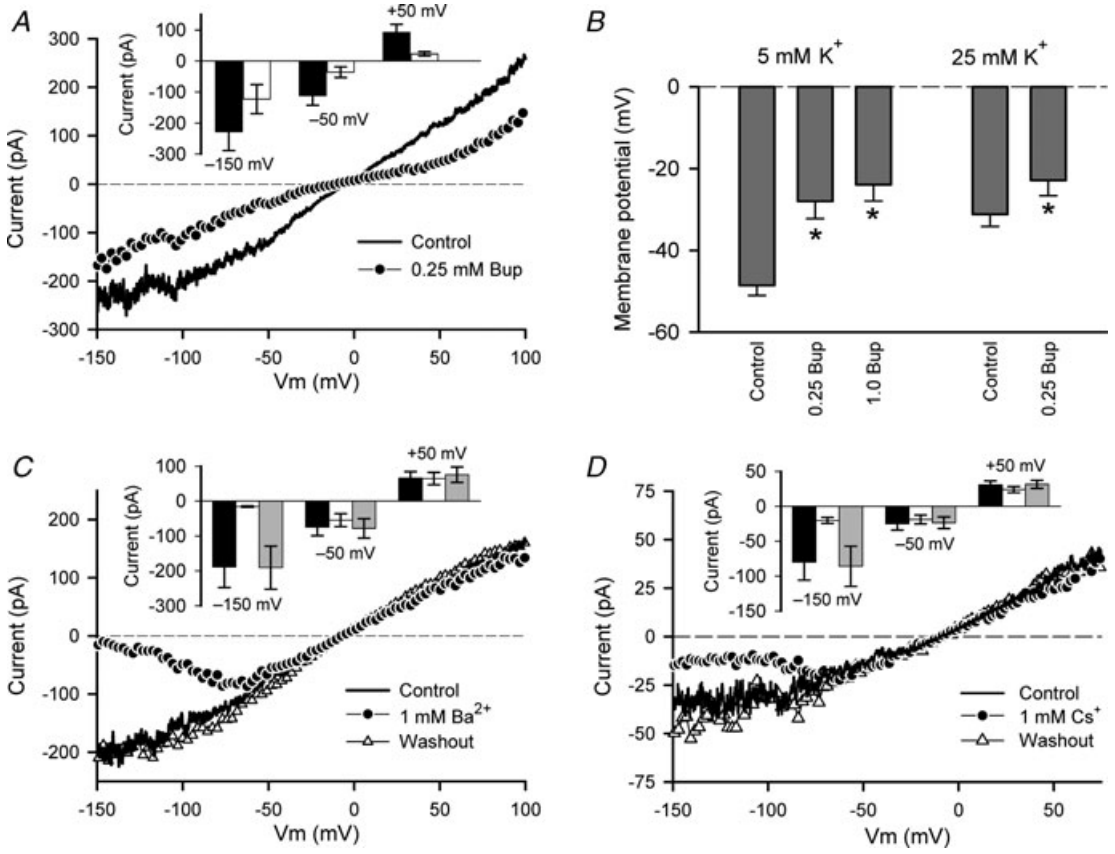

Figure 8. Pharmacological properties of background K^+ current
A, effect of 0.25 mM bupivacaine (Bup) on background K^+ current *I–V* relation. A ramp voltage-clamp protocol was used to generate the *I–V* relation. External $[K^+]$ was 145 mM, pH_o was 8.5. Inset shows plot of current magnitude (±SEM) at −150, −50 and +50 mV, in control (black) and with 0.25 mM Bup (white). Data pooled from 9 cells. *B*, effect of 0.25 and 1 mM Bup on RMP of HAC in 5 ($n = 8$) and 25 mM ($n = 5$) external K^+. For 5 mM K^+, * indicates significant differences ($P < 0.001$) compared with control (C); there was no significant difference between 0.25 and 1.0 mM Bup (repeated measures ANOVA). For 0.25 mM Bup in 25 mM K^+, $P = 0.0127$, paired *t* test. *C*, effect of 1 mM Ba^{2+} on background K^+ current (ramp protocol) *I–V* relation. External $[K^+]$ was 145 mM, pH_o was 8.5. Ba^{2+} blocked the K^+ current in a voltage-dependent, reversible manner. Inset shows current magnitude at three membrane potentials of the *I–V* relation, −150, −50 and +50 mV, in control (black), with 1 mM Ba^{2+} (white), and after washout of Ba^{2+} (grey). Data pooled from 4 cells. *D*, effect of 1 mM Cs^+ on background K^+ current (ramp protocol) *I–V* relation. External $[K^+]$ was 145 mM, and pH_o was 7.4. Inset shows current magnitude at three membrane potentials of the *I–V* relation, −150, −50 and +50 mV, in control (black), with 1 mM Cs^+ (white), and after washout of Cs^+ (grey). Data pooled from 5 cells.

voltage-gated K^+ channels were identified in HACs. The first, observed in approximately 50% of cells, was a time- and potential-dependent delayed rectifier current (e.g. Figs 2 and 3). This current activated near –40 mV, and increased in magnitude and rate of activation with membrane depolarization. This current was blocked by α-DTX (Fig. 4), which is a selective blocker of time- and voltage-dependent K^+ currents produced by $K_v1.1$, $K_v1.2$ and $K_v1.6$ channels (Harvey & Robertson, 2004). Neonatal mouse articular chondrocytes express a voltage-gated K^+ current with qualitatively similar properties to the delayed rectifier current recorded from HACs (Clark *et al.* 2010). The K^+ current in mouse articular chondrocytes (ACs) was 50% blocked by 20 nM of α-DTX. This current was probably produced in mouse ACs by Kv1.6 K^+ channels, based on high expression levels of mRNA for KCNA6 and Kv1.6 protein. The sensitivity of the delayed rectifier current in HACs to α-DTX suggests that Kv1.6 K^+ channels may at least partly underlie this current. Adult rat ACs (Ponce, 2006) express a voltage-gated K^+ current that is blocked by α-DTX, as well as charybdotoxin and margatoxin. However, expression levels of K^+ channel transcripts that might underlie the current were not reported.

Another prominent K^+ current that was expressed in virtually all HACs was characterized by large fluctuations or 'noise' and was activated near +50 mV, increasing very steeply in magnitude with further membrane depolarization (e.g. Figs 2 and 3). The current was sensitive to relatively low concentrations of TEA ($K_d = 0.15$ mM), and was partially (~50%) blocked by 100 nM IbTX, but was insensitive to 100 nM α-DTX. These electrophysiological and pharmacological data and the robust expression of *KCNMA1* mRNA and K^+ channel α-subunit protein in HACs strongly suggest that the 'noisy' outward current was produced by large-conductance Ca^{2+}-activated, BK channels. Although free $[Ca^{2+}]$ in the pipette solution was very low (pCa ~7.9), activation of BK channels is regulated by both internal Ca^{2+} concentration and membrane potential (Magleby, 2003). BK-like K^+ channels have previously been identified in equine articular chondrocytes using both electrophysiological and immunohistological techniques (Mobasheri *et al.* 2010).

Voltage-gated delayed rectifier-like K^+ channels do not appear to contribute significantly to RMP of isolated HACs under our culture and electrophysiological recording conditions. The mean RMP of cells expressing delayed rectifier current was not significantly different from that of cells lacking this current. In addition, blocking the delayed rectifier K^+ current with 5 mM TEA had very little effect on RMP in 5 mM external K^+. These findings differ from those in isolated rat, mouse and canine articular chondrocytes. In both canine and mouse articular chondrocytes, TEA blocked a delayed rectifier K^+ current and resulted in a concomitant membrane depolarization (Wilson *et al.* 2004; Clark *et al.* 2010). Similarly, TEA, 4-aminopyridine, charybdotoxin and α-dendrotoxin all blocked voltage-gated delayed rectifier-like K^+ currents in rat articular chondrocytes, and produced substantial depolarization of these cells (Ponce, 2006). A reason for the apparent discrepancy between these data from HACs and the other mammalian articular chondrocytes may be due to the very small magnitude of the delayed rectifier K^+ currents in HACs, as compared with similar currents in rat, mouse and canine chondrocytes. The average delayed rectifier current in HACs, measured as the α-DTX-sensitive current (Fig. 4), appeared to be too small at the RMP (in 5 mM K^+) to significantly influence membrane potential. Based on the magnitude and membrane potential dependence of activation of the α-DTX-sensitive current (Fig. 4), the average current produced by the delayed rectifier was estimated from the best-fit Boltzmann function to be ~0.1 pA (for a 7 pF cell) at –45 mV, which was near the average RMP of HACs that expressed a delayed rectifier current. Even though the cell input resistance near RMP was ~11 GΩ, this very small current would be expected to have no perceptible effect on RMP.

K_{2p} K^+ channels in human articular chondrocytes

Changes in external K^+ concentration and pH revealed the presence of a distinct K^+ current in isolated HACs which had characteristics that were consistent with those of K^+ currents produced by two-pore domain K^+ channels. Transcripts for three *KNCK* genes, namely *KCNK1*, *KCNK5* and *KCNK6*, were expressed at substantial levels in HACs. The protein products of these genes correspond to 'TWIK-1', 'TASK-2' and TWIK-2' K_{2p} K^+ channels, respectively. Identification of the K_{2p} K^+ channel or channels underlying the background K^+ current in HACs is complicated by the lack of highly specific activators and/or inhibitors of these channels. However, the K_{2p} K^+ channels resulting from the three highly expressed *KCNK* genes have distinctly different properties, particularly their responses to changes in external pH.

It has been reported that the related TWIK-1 and TWIK-2 K_{2p} channels express weakly inward rectifying K^+ currents when heterologously expressed in *Xenopus* oocytes (Lesage *et al.* 1996; Chavez *et al.* 1999). However, others have reported lack of functional TWIK-1 K^+ currents in the same expression system (Goldstein *et al.* 1998). There are similarly conflicting reports on functional expression of TWIK-2 channels in *Xenopus* oocytes, with one group describing membrane currents with biophysical properties similar to those of TWIK-1 channels (Chavez *et al.* 1999), while another group did not see functional expression in *Xenopus* oocytes or HEK293T

cells (Pountney *et al.* 1999). A third group described functional expression of inactivating human and rat TWIK-2 currents in transiently transfected COS-7 cells (Patel *et al.* 2000), although *KCNK6* cloned from mouse failed to produce K^+ currents in the same expression system (Lloyd *et al.* 2009).

In those studies where TWIK-1 and TWIK-2 K^+ currents were expressed, three properties of these currents differed significantly from the properties of the background K^+ current in HACs. First, although both TWIK-1 and TWIK-2 currents were blocked by relatively low concentrations of Ba^{2+}, the efficacy of block was dependent on external K^+ concentration. For example, although TWIK-1 and TWIK-2 were blocked by Ba^{2+} with an approximate IC_{50} of 100 μM in 5 mM external K^+ (Lesage *et al.* 1996; Patel *et al.* 2000), TWIK-2 was insensitive to 1 mM Ba^{2+} in elevated external K^+ (Chavez *et al.* 1999; Patel *et al.* 2000). Moreover, block of TWIK-2 by Ba^{2+} was reported to be voltage-independent (Lloyd *et al.* 2009). These data are inconsistent with the properties of the background K^+ current of HAC, which was blocked in a strongly voltage-dependent manner by Ba^{2+} (1 mM) in high external K^+ concentrations (e.g. 145 mM; Fig. 8). Second, many K_{2p} channels are blocked by bupivacaine at submillimolar doses, but unlike HAC background K^+ current, TWIK-1 and TWIK-2 were relatively insensitive to this local anaesthetic (Kindler *et al.* 2003). A third property in which HAC background current differs from that of TWIK-1 and TWIK-2 currents is the sensitivity of HAC current to external pH. In contrast, both TWIK-1 and TWIK-2 are inhibited by internal, but not external acidification (Lesage *et al.* 1996; Chavez *et al.* 1999). All of these differences between the properties of TWIK-1/TWIK-2 K^+ currents and HAC background K^+ current strongly suggest that despite substantial expression of *KCNK1* and *KCNK6* mRNA, the associated K_{2p} channels, if expressed in HACs, probably contribute little to the background K^+ current.

KCNK5 is the third two-pore domain K^+ channel gene that was expressed at substantial quantities in isolated HACs. Of the three *KCNK* K^+ channels expressed in HACs, the properties of HAC background current most closely resemble those of TASK-2, the *KCNK5* ion channel. TASK-2 currents are inhibited by acidic pH_o, with a p*K* of approximately 8 (Reyes *et al.* 1998; Niemeyer *et al.* 2001). The large increase in background K^+ current recorded in HACs in response to an increase in pH_o from 7.4 to 8.5 (Fig. 7) is consistent with this rather alkaline p*K*. The sensitivity of HAC background current to pH_o does not depend on external $[K^+]$, as shown by the data in Fig. 7*C*, where elevated pH_o produced similar increases in membrane conductance in 25 and 145 mM external K^+. This is consistent with the properties of TASK-2 channels. The volume-sensitive K^+ current in Ehrlich ascites tumour cells, which has been shown to very likely be produced by TASK-2 channels (Niemeyer *et al.* 2001), is equally sensitive to pH_o in 5 and 95 mM external K^+ (Hougaard *et al.* 2001). This differs markedly from the properties of another pH_o-sensitive K_{2p} channel, TASK-1 (*KCNK3*), for which elevated external $[K^+]$ abolished effects of pH_o on current magnitude (Lopes *et al.* 2000). TASK-2 was reported to be relatively insensitive to Ba^{2+} and Cs^+ (Reyes *et al.* 1998), based on the effect of these cations on current measured at a membrane potential of +50 mV. However, testing at this single positive potential would miss the strong voltage dependence of block by $Ba^{2+}$and Cs^+ as shown for HAC background current in Fig. 8. Other K_{2p} channels, such as TASK-1, are blocked by Ba^{2+} and Cs^+ in a similar voltage-dependent manner (O'Connell *et al.* 2005). Bupivacaine is a potent blocker of TASK-2 channels (Reyes *et al.* 1998), but the block was reported to be virtually independent of membrane potential (Kindler *et al.* 2003). This appears to differ from the effect of bupivacaine on HAC background current, which is voltage-dependent. Although the expression of *KNCK5* RNA and TASK-2 α-subunits is alone not sufficient to guarantee production of a membrane current, the biophysical and pharmacological properties of the background current in HACs most closely resemble those of TASK-2 K^+ channels.

Bupivacaine and chondrotoxicity

The local anaesthetic bupivacaine is widely used as an analgesic following joint surgery, but questions have been raised about its possible role in articular chondrolysis, especially during chronic application, e.g. using intra-articular infusion pumps (Busfield & Romero, 2009; Webb & Ghosh, 2009). Deleterious effects of bupivacaine on human and bovine articular chondrocytes have been shown *in vitro* following short (as little as 15 min) exposures to clinical concentrations of the drug (Chu *et al.* 2008; Lo *et al.* 2009). At least part of the damage to chondrocytes produced by bupivacaine and the related drugs lidocaine and ropivacaine is likely to be due to damage to the mitochondrial genome, possibly resulting in loss of energy production and induction of apoptosis (Grishko *et al.* 2010). However, disruption of intracellular Ca^{2+} homeostasis might also play a role in the drug-induced damage. Changes in membrane potential can result in changes in intracellular $[Ca^{2+}]$ in chondrocytes. For example, membrane hyperpolarization resulting from activation of K^+ channels or blocking of 'resting' Cl^- channels produces increased Ca^{2+} entry in chondrocyte-like OUMS-27 cells (Funabashi *et al.* 2010*a*,*b*). Hypertonic shock increases internal $[Ca^{2+}]$ of bovine articular chondrocytes, but this was abolished if the accompanying membrane hyperpolarization was also blocked (Sánchez & Wilkins, 2004). Membrane

depolarization produced in HACs by block of TASK-2 K^+ channels by bupivacaine (Fig. 8) might also contribute to an alteration in intracellular Ca^{2+} homeostasis. Although membrane depolarization would be expected to reduce the driving force for Ca^{2+} entry into the chondrocyte, this same depolarization might impair the efficacy of the Na^+–Ca^{2+} exchanger, which is an important transport mechanism contributing to intracellular Ca^{2+} homoeostasis in chondrocytes (Sánchez & Wilkins, 2004). Reduction of the electrochemical potential for forward mode operation of the exchanger (i.e. Ca^{2+} extrusion) by membrane depolarization might result in changes in intracellular $[Ca^{2+}]$.

Physiological role for TASK-2 channels in HACs

TASK-2 channels have been implicated in stabilizing RMP of a diverse variety of cells, for example rat pulmonary arteries (Gönczi *et al.* 2006), mouse urinary bladder smooth muscle (Beckett *et al.* 2008), retinal glial (Müller) cells (Skatchkov *et al.* 2006) and brainstem chemoreceptive cells involved in central respiratory CO_2 and O_2 sensitivity (Gesteau *et al.* 2010). The data presented here show that K_{2p} K^+ channels, probably TASK-2, can contribute significantly to maintaining RMP of HACs under cell culture conditions, but the role these channels may play *in situ* in the intact cartilage is unclear. The activity of a number of ion channels in HACs is influenced by the mechanical and osmotic forces produced during compression and relaxation of the cartilage that accompanies movement of articular joints. Mechanical and osmotic forces on chondrocytes result in increases in internal $[Ca^{2+}]$ (Yellowley *et al.* 1997, 2002; Sánchez & Wilkins, 2004), which has the potential to activate Ca^{2+}-sensitive K^+ channels, such as BK and SK channels (Wright *et al.* 1996; Mobasheri *et al.* 2010). Mechanical and osmotic forces can open stretch-activated non-selective ion channels such as transient receptor potential channels, e.g. TRPV4 (Phan *et al.* 2009) and volume-sensitive Cl^- channels (Isoya *et al.* 2009). 'Resting' Cl^- channels can contribute significantly to RMP in human cell-line chondrocytes *in vitro* (Funabashi *et al.* 2010*a*). The membrane potential of a chondrocyte will therefore depend on the relative magnitudes of the various active ion conductances, some of which are probably varying moment to moment during normal movement of the articular joint. Hence, the influence of the TASK-2 K^+ current on RMP will depend on its magnitude in relation to other active ionic currents. As TASK-2 currents are small, they may have the greatest influence on membrane potential when the chondrocytes are under least mechanical and osmotic forces, i.e. in articular joints at 'rest', when mechano- and osmosensitive ion channels would be likely to be least activated.

References

Barrett-Jolley R, Lewis R, Fallman R & Mobasheri A (2010). The emerging chondrocyte channelome. *Front Physio* **1**, 135.

Beckett EA, Han I, Baker SA, Han J, Britton FC & Koh SD (2008). Functional and molecular identification of pH-sensitive K^+ channels in murine urinary bladder smooth muscle. *BJU Int* **102**, 113–124.

Busfield BT & Romero DM (2009). Pain pump use after shoulder arthroscopy as a cause of glenohumeral chondrolysis. *Arthroscopy* **25**, 647–652.

Chavez RA, Gray AT, Zhao BB, Kindler CH, Mazurek MJ, Mehta Y, Forsayeth JR & Yost CS (1999). TWIK-2, a new weak inward rectifying member of the tandem pore domain potassium channel family. *J Biol Chem* **274**, 7887–7892.

Chu CR, Izzo NJ, Coyle CH, Papas NE & Logar A (2008). The *in vitro* effects of bupivacaine on articular chondrocytes. *J Bone Joint Surg Br* **90**, 814–820.

Clark RB, Hatano N, Kondo C, Belke DD, Brown BS, Kumar S, Votta BJ & Giles WR (2010). Voltage-gated K^+ currents in mouse articular chondrocytes regulate membrane potential. *Channels* **4**, 179–191.

Eilam Y, Beit-Or A & Nevo Z (1985). Decrease in cytosolic free Ca^{2+} and enhanced proteoglycan synthesis induced by cartilage derived growth factors in cultured chondrocytes. *Biochem Biophys Res Comm* **132**, 770–779.

Fassbender HG (1987). Role of chondrocytes in the development of osteoarthritis. *Am J Med* **83**, 17–24.

Funabashi K, Fujii M, Yamamura H, Ohya S & Imaizumi Y (2010*a*). Contribution of chloride channel conductance to the regulation of resting membrane potential in chondrocytes. *J Pharmacol Sci* **113**, 94–99.

Funabashi K, Ohya S, Yamamura H, Hatano N, Muraki K, Giles W & Imaizumi Y (2010*b*). Accelerated Ca^{2+} entry by membrane hyperpolarization due to Ca^{2+}-activated K^+ channel activation in response to histamine in chondrocytes. *Am J Physiol Cell Physiol* **298**, C786–797.

Gestreau C, Heitzmann D, Thomas J, Dubreuil V, Bandulik S, Reichold M, Bendahhou S, Pierson P, Sterner C, Peyronnet-Roux J, Benfriha C, Tegtmeier I, Ehnes H, Georgieff M, Lesage F, Brunet JF, Goridis C, Warth R & Barhanin J (2010). Task2 potassium channels set central respiratory CO_2 and O_2 sensitivity. *Proc Natl Acad Sci U S A* **107**, 2325–2330.

Goldstein SAN, Bayliss DA, Kim D, Lesage F, Plant LD & Rajan S (2005). International Union of Pharmacology. LV. Nomenclature and molecular relationships of two-P potassium channels. *Pharmacol Rev* **57**, 527–540.

Goldstein SAN, Bockenhauer D, O'Kelly I & Zilberberg N (2001). Potassium leak channels and the KCNK family of two-P-domain subunits. *Nat Rev Neurosci* **2**, 175–184.

Goldstein SAN, Wang KW, Ilan N & Pausch MH (1998). Sequence and function of the two P domain potassium channels: implications of an emerging superfamily. *J Mol Med* **76**, 13–20.

Gönczi M, Szentandrássy N, Johnson IT, Heagerty AM & Weston AH (2006). Investigation of the role of TASK-2 channels in rat pulmonary arteries; pharmacological and functional studies following RNA interference procedures. *Br J Pharmacol* **147**, 496–505.

Gray ML, Pizzanelli AM, Grodzinsky AJ & Lee RC (1988). Mechanical and physiochemical determinants of the chondrocyte biosynthetic response. *J Orthop Res* **6**, 777–792.

Grishko V, Xu M, Wilson G & Pearsall AW 4th (2010). Apoptosis and mitochondrial dysfunction in human chondrocytes following exposure to lidocaine, bupivacaine and ropivacaine. *J Bone Joint Surg Am* **92**, 609–618.

Harvey AL & Robertson B (2004). Dendrotoxins: structure-activity relationships and effects on potassium ion channels. *Curr Med Chem* **11**, 3065–3072.

Hougaard C, Jørgensen F & Hoffmann EK (2001). Modulation of the volume-sensitive K^+ current in Ehrlich ascites tumour cells by pH. *Pflugers Arch* **442**, 622–633.

Isoya E, Toyoda F, Imai S, Okumura N, Kumagai K, Omatsu-Kanbe M, Kubo M, Matsuura H & Matsusue Y (2009). Swelling-activated Cl^- current in isolated rabbit articular chondrocytes: inhibition by arachidonic acid. *J Pharmacol Sci* **109**, 293–304.

Kindler CH, Paul M, Zou H, Liu C, Winegar BD, Gray AT & Yost CS (2003). Amide local anesthetics potently inhibit the human tandem pore domain background K^+ channel TASK-2 (KCNK5). *J Pharmacol Exp Ther* **306**, 84–92.

Kindler CH & Yost CS (2005). Two-pore domain potassium channels: new sites of local anesthetic action and toxicity. *Reg Anesth Pain Med* **30**, 260–274.

Lesage F, Guillemare E, Fink M, Duprat F, Lazdunski M, Romey G & Barhanin J (1996). TWIK-1, a ubiquitous human weakly inward rectifying K^+ channel with a novel structure. *EMBO J* **15**, 1004–1011.

Lesage F & Lazdunski M (2000). Molecular and functional properties of two-pore-domain potassium channels. *Am J Physiol Renal Physiol* **279**, F793–F801.

Lloyd EE, Marrelli SP, Namiranian K & Bryan RM (2009). Characterization of TWIK-2, a two-pore domain K^+ channel, cloned from the rat middle cerebral artery. *Exp Biol Med* **234**, 1493–1502.

Lo IKY, Sciore P, Chung M, Liang S, Boorman RB, Thornton GM, Rattner JB & Muldrew K (2009). Local anesthetics induce chondrocyte death in bovine articular cartilage disks in a dose- and duration-dependent manner. *Arthroscopy* **25**, 707–715.

Lopes CMB, Gallagher PG, Buck ME, Butler MH & Goldstein SAN (2000). Proton block and voltage gating are potassium-dependent in the cardiac leak channel Kcnk3. *J Biol Chem* **275**, 16969–16978.

Magleby KL (2003). Gating mechanism of BK (Slo1) channels: so near, yet so far. *J Gen Physiol* **121**, 81–96.

Mobasheri A, Dart C & Barrett-Jolley R (2008). Potassium ion channels in articular chondrocytes. Putative roles in mechanotransduction, metabolic regulation and cell proliferation. In *Mechanosensitive Ion Channels*, ed. Kamkin A & Kiseleva I, pp. 157–178. Springer, Berlin.

Mobasheri A, Lewis R, Maxwell JEJ, Hill C, Womack M & Barrett-Jolley R (2010). Characterization of a stretch-activated potassium channel in chondrocytes. *J Cell Physiol* **223**, 511–518.

Mouw JK, Imler SM & Levenston ME (2007). Ion-channel regulation of chondrocyte matrix synthesis in 3D culture under static and dynamic compression. *Biomech Model Mechanobiol* **6**, 33–41.

Muir H (1995). The chondrocyte, architect of cartilage. Biomechanics, structure, function and molecular biology of cartilage matrix macromolecules. *Bioessays* **17**, 1039–1048.

Neher E (1992). Correction for liquid junction potentials in patch clamp experiments. In *Methods in Enzymology*, vol. 207, Ion Channels, ed. Ruby B & Iverson LE, pp. 123–131. Academic Press, San Diego.

Niemeyer MI, Cid LP, Barros LF & Sepúlveda FV (2001). Modulation of the two-pore domain acid-sensitive K^+ channel TASK-2 (KCNK5) by changes in cell volume. *J Biol Chem* **276**, 43166–43174.

O'Connell AD, Morton MJ, Sivaprasadarao A & Hunter M (2005). Selectivity and interactions of Ba^{2+} and Cs^+ with wild-type and mutant TASK1 K^+ channels expressed in *Xenopus* oocytes. *J Physiol* **562**, 687–696.

Patel AJ & Honoré E (2001). Properties and modulation of mammalian 2P domain K^+ channels. *Trends Neurosci* **24**, 339–346.

Patel AJ, Maingret F, Magnone V, Fosset M, Lazdunski M & Honoré E (2000). TWIK-2, an inactivating 2P domain K^+ channel. *J Biol Chem* **275**, 28722–28730.

Phan MN, Leddy HA, Votta BJ, Kumar S, Levy DS, Lipshutz DB, Lee SH, Liedtke W & Guilak F (2009). Functional characterization of TRPV4 as an osmotically sensitive ion channel in porcine articular chondrocytes. *Arthritis Rheum* **60**, 3028–3037.

Ponce A (2006). Expression of voltage dependent potassium currents in freshly dissociated rat articular chondrocytes. *Cell Physiol Biochem* **18**, 35–46.

Pountney DJ, Gulkarov I, Vega-Saenz de Miera E, Holmes D, Saganich M, Rudy B, Artman M & Coetzee WA (1999). Identification and cloning of TWIK-originated similarity sequence (TOSS): a novel human 2-pore K^+ channel principal subunit. *FEBS Lett* **450**, 191–196.

Reyes R, Duprat F, Lesage F, Fink M, Salinas M, Farman N & Lazdunski M (1998). Cloning and expression of a novel pH-sensitive two pore domain K^+ channel from human kidney. *J Biol Chem* **273**, 30863–30869.

Sánchez JC & Wilkins RJ (2004). Changes in intracellular calcium concentration in response to hypertonicity in bovine articular chondrocytes. *Comp Biochem Physiol A Mol Integr Physiol* **137**, 173–182.

Skatchkov SN, Eaton MJ, Shuba YM, Kucheryavykh YV, Derst C, Veh RW, Wurm A, Iandiev I, Pannicke T, Bringmann A & Reichenbach A (2006). Tandem-pore domain potassium channels are functionally expressed in retinal (Müller) glial cells. *Glia* **53**, 266–276.

Urban JP, Hall AC & Gehl KA (1993). Regulation of matrix synthesis rates by the ionic and osmotic environment of articular chondrocytes. *J Cell Physiol* **154**, 262–270.

Webb ST & Ghosh S (2009). Intra-articular bupivacaine: potentially chondrotoxic? *Br J Anaesth* **102**, 439–441.

Wilkins RJ & Hall AC (1995). Control of matrix synthesis in isolated bovine chondrocytes by extracellular and intracellular pH. *J Cell Physiol* **164**, 474–481.

Wilson JR, Duncan NA, Giles WR & Clark RB (2004). A voltage-dependent K^+ current contributes to membrane potential of acutely isolated canine articular chondrocytes. *J Physiol* **557**, 93–104.

Wohlrab D, Vocke M, Klapperstück T & Hein W (2005). The influence of lidocaine and verapamil on the proliferation, CD44 expression and apoptosis behavior of human chondrocytes. *Int J Mol Med* **16**, 149–157.

Wohlrab D, Wohlrab J, Reichel H & Hein W (2001). Is the proliferation of human chondrocytes regulated by ionic channels? *J Orthop Sci* **6**, 155–159.

Wright M, Jobanputra P, Bavington C, Salter DM & Nuki G (1996). Effects of intermittent pressure-induced strain on the electrophysiology of cultured human chondrocytes: evidence for the presence of stretch-activated membrane ion channels. *Clin Sci (Lond)* **90**, 61–71.

Wu QQ & Chen Q (2000). Mechanoregulation of chondrocyte proliferation, maturation and hypertrophy: ion-channel dependent transduction of matrix deformation signals. *Exp Cell Res* **256**, 383–391.

Yellowley CE, Hancox JC & Donahue HJ (2002). Effects of cell swelling on intracellular calcium and membrane currents in bovine articular chondrocytes. *J Cell Biochem* **86**, 290–301.

Yellowley CE, Jacobs CR, Li Z, Zhou Z & Donahue HJ (1997). Effects of fluid flow on intracellular calcium in bovine articular chondrocytes. *Am J Physiol Cell Physiol* **42**, C30–C36.

Author contributions

R.B.C.: conception and design of experiments, collection, analysis and interpretation of all electrophysiological data, and drafting and revising the manuscript. C.K.: cell preparation and culture, RNA isolation, immunocytological sample preparation and image collection. D.B.: qRT-PCR data collection, and interpretation. W.R.G.: critical revision of the manuscript. All authors have approved the final version of the manuscript.

Acknowledgements

This project was funded by a research grant to W.R.G. from the Canadian Institutes of Health Research, and a Scientist Award from Alberta Innovates – Health Solutions. Dr R. Krawetz (Department of Surgery, University of Calgary) and Ms S. Hunter (Alberta Bone and Joint Health Institute, University of Calgary) are thanked for supplying cartilage samples.